Report

Reference Material

BAM-N010

Hydrodynamic Equivalent Sphere Diameter of Polypropylene Nanoparticles

August 2026

Coordinator: Andreas F. Thünemann

Bundesanstalt für Materialforschung und -prüfung (BAM)

Division 6.5 Synthesis and Scattering of Nanostructured Materials

Unter den Eichen 87

12205 Berlin, Germany

Phone: +49 30 8104 1610

E-Mail: andreas.thuenemann@bam.de

Summary

This report describes the preparation and analysis of the reference material BAM-N010, specifically the hydrodynamic diameter of polypropylene nanoparticles, encompassing all analytical aspects and providing evidence of homogeneity and stability. Dynamic light scattering (DLS) was used to characterize the hydrodynamic diameter of the particles in accordance with the ISO 22412 standard. The reference value for D_h and its expanded uncertainty U are summarized in the table below. This report provides detailed information on preparing the reference material as well as homogeneity and stability investigations.

Property	Value[1]	U [2]	Unit
Hydrodynamic diameter (D_h)	174	26	nm

1. Values are means from the values of the characterization study.
2. Expanded uncertainty $U = k\ u_c$ was calculated according to ISO 33405 [1] with a coverage factor $k = 2$, providing a level of confidence of approximately 95%. The value of the combined standard uncertainty u_c of the property includes an uncertainty contribution resulting from the study of the homogeneity and stability of the material.

Contents

1 Introduction 4

2 Manufacture of BAM-N010 6

2.1 Materials 6
2.2 Preliminary studies 6
2.3 Synthesis of polypropylene nanoparticles 7
2.4 Preparation of reference material 8

3 Characterization 8

4 Homogeneity 10

5 Stability 13

6 Combined uncertainty 15

7 Supporting Information 16

7.1 Concentration 16
7.2 Experimental for determination of hydrodynamic diameter, PDI, and zeta potential 16
7.3 Data of long-term stability study 17
7.4 Heat sterilization. 21
7.5 Scanning electron microscopy (SEM) 22

8 Information on the proper use of the RM 23

8.1 Recommended use 23
8.2 Transport, storage, and handling 23
8.3 Shelf-life 24
8.4 Safety information 24

9 Information on and purchase of the RM 24

10 References 25

11 Annexes 26

11.1 Information about the software utilized 26
11.2 Acknowledgment 26

List of abbreviations

(if not explained elsewhere)

RM	reference material
DLS	dynamic light scattering
df	degrees of freedom
F	Fisher statistic
F_{crit}	critical value of the Fisher distribution
M	mean square
$M_{between}$	mean square between groups
M_{within}	mean square within group
MS	mean squared error
N	number of bottles
n	number of replicate determinations
SS	sum of squares
s	standard deviation
s_{bb}	between-unit standard deviation
s_r	repeatability standard deviation
u_{hom}	uncertainty caused by inhomogeneity
u_{char}	uncertainty caused by characterization
u_{lts}	uncertainty caused by instability

1 Introduction

Plastic nanoparticles, also known as nanoplastics, are believed to be becoming more common in nature [2]. This is because global plastic production is rising, and waste is not being disposed of properly in many parts of the world [3]. There are no effective strategies for completely reusing or recycling plastics, thereby preventing them from entering the environment. Only about 21% of plastic produced from 1950 to 2015 has been recycled or incinerated, leaving 79% that has ended up in landfills or entered the natural environment through other means [4]. Different degradation processes break down macroplastics into microplastics, which finally degrade into nanoplastics. Awareness of these processes and the potentially harmful effects of microplastics is evident today. For clarity, it should be noted that in addition to the international report ISO/TR21960:2020, Hartmann et al. have suggested that nanoplastics particles refer to dimensions < 1 µm [5]. We refer to both publications for definitions

and classifications of plastic debris. In contrast, Sieg et al. have decided to use the term “nano” as commonly used in the nanotoxicology field, i.e., particles ranging in size from 1 to 100 nanometers [6]. In literature, a gap often exists in the definition between the lower size limit for microplastics (>1 µm) and the upper size limit for nanoparticles (<100 nm). For the plastic particles with diameters between 100 and 1000 nm, the term “submicron” is often used [6]. For clarity, here we refer to polymer nanoparticles as plastic particles in the size range of 1 nm to 1 µm.

Paul-Pont et al. recommended conducting laboratory studies on microplastics made from the ‘Big Six” polymers, i.e., polypropylene (PP), polyethylene (PE), polyvinyl chloride (PVC), polyurethane (PU), polyethylene terephthalate (PET), and polystyrene (PS), so that priorities could be set for experimentally exposing marine organisms to these plastics [7]. These polymers account for approximately 80% of the plastics produced in the European Union. Special attention can be given to polypropylene and polyethylene, as their recovery rates are the highest across all environmental compartments. For example, polyethylene makes up 53-67%, and polypropylene accounts for 16-30% of the plastics in the Bay of Brest [8]. Due to the limited data on nanoplastics, we assume that polyethylene and polypropylene are equally prevalent as nanoplastics.

Unlike microplastics, data on nanoplastics is limited [9]. This also means that the risk assessment of nanoplastics is still in its early stages. However, some studies present essential reasons for concern. For example, Tallec et al. discovered that nanoplastics caused a significant decrease in fertilization success and embryo-larval development in Pacific oysters, while no effects from plain microplastics were observed [10]. Hollóczki and Gehrke reported that polyethylene nanoparticles dissolve in the hydrophobic core of lipid bilayers in a simulation study [11]. Consequently, there is also a risk that essential functions of cell membranes might be affected. The same authors reported that nanoplastics can alter the secondary structure of proteins [12]. In this case, the danger is that such proteins might lose their function, with enzymes potentially becoming inactive, for example.

This report details the production and characterization of long-term stable aqueous dispersions of polypropylene nanoparticles derived from bulk material. The described method for preparing polypropylene nanoparticles was inspired by the approach proposed by Ekvall, who formed nanoplastics by mechanically breaking down polystyrene products used in daily life [13]. The authors generated polystyrene nanoplastics directly in water with a household immersion blender. Ekvall et al. also recently reported on high-density polyethylene nanoplastics with a diameter of around 110 nm, which caused a size-dependent toxic effect in the zooplankton species Daphnia magna [14]. In their method, the prepared polyethylene particles were unstable in solution over time, resulting in no nanoparticles being detected after 100 days of storage. Very likely, their zeta potential of approximately -10.9 ± 6.4 mV was insufficient to ensure long-term colloidal stability. Long-term stable particles are expected when zeta potentials are below -30 mV [15]. Since we aimed to avoid using surfactant stabilizers, achieving a strongly negative zeta potential was the primary goal for ensuring colloidally stable dispersions. Below, we demonstrate

how this was achievable for polypropylene nanoparticles. These dispersions are intended as reference materials for detecting nanoplastics in liquid samples. Such reference materials could assist in developing methods to detect polypropylene nanoplastics in food and environmental samples. We have published many physicochemical details on polypropylene nanoparticles elsewhere [16]. This includes the question of their behavior in solutions with different salt concentrations. The following addresses only aspects related to the properties as a reference material.

2 Manufacture of BAM-N010

2.1 Materials

All chemicals were used as received without further purification. Polypropylene (isotactic, M_w ≈ 12000 g mol^{-1}, Mn ≈ 5000 g mol^{-1}) was purchased from Sigma Aldrich. Acetone (p.a., min. 99.5%, ChemSolute) was purchased from Th. Geyer. The water for preparation was purified using a Sartorius arium 611 DI purifier. Folded filters of grade 2105 (fast filtering, particle retention 12 µm - 15 µm, by LabSolute) were purchased from Th. Geyer.

2.2 Preliminary studies

Mechanical breakdown was employed to crush macroscopic polypropylene granules into smaller pieces using a mechanical disperser based on the rotor-stator principle, thereby providing a higher mechanical energy input than that used by Ekvall [13]. Preparing polypropylene nanoparticles directly in water proved unsuccessful; however, success was achieved when using acetone as the dispersion medium, with the polypropylene granules crushed at 0 °C. Larger polymer fragments were removed after mechanical breakdown via filtration. Then water was added, and the acetone was finally removed by distillation (see Section 2.3 for details). In the form of dispersion, it remains as an aqueous phase, exhibiting the typical semi-transparent appearance of a diluted particle dispersion, as shown in Figure 1. We assume that polypropylene is brittle enough under the chosen conditions to form a significant number of separated nanoparticles, which are simultaneously stabilized through colloid stabilization. We also think that processes such as polymer welding, which counteract nanoparticle formation, predominate in pure water. As such, polypropylene nanoparticles do not form in water without surfactants. Lionetto et al. reported the production of PET nanoparticles through a stepwise grinding and sieving process of PET pellets [17]. Like our observations, their work also suggests that high mechanical energy input typically causes nanoparticles to re-weld if they are not immediately stabilized through colloid formation. Polystyrene, on the other hand, is brittle at ambient conditions, which may explain why re-welding processes failed to prevent the formation of PS nanoparticles in Ekvall's study [13]. It seems plausible that the formation of nanoparticles by grinding becomes more difficult as the glass transition temperature of the polymer increases. The glass transition depends not only

on the material but also on how the polymer is pretreated. Nevertheless, the glass transition temperature and thereby the ease of preventing re-welding increase in the order PE (-100 °C), PP (-10 °C), PET (70 °C), to PS (100 °C).

Since our polypropylene nanoparticles are dispersed in pure water without any added stabilizer, we assumed that the particles would start to agglomerate after short periods of storage. To test this, a sample was placed in a glass vial and kept at room temperature under normal lighting conditions for a month. Surprisingly, no signs of agglomeration were observed in the DLS data. This suggests that no additional stabilizing surfactants are needed to achieve a long-term stable aqueous dispersion of polypropylene nanoparticles. Therefore, the idea that this method might be suitable for producing a reference material appears justified.

The particle preparation was suspended in acetone because acetone does not form an azeotrope with water [18], and it can be easily removed from an acetone/water mixture by evaporation due to its low boiling point of 56°C. There was a possibility that the polypropylene chains had been mechanochemically cleaved, and that the acetone might have reacted with the subsequently produced polymer fragments. For this reason, gel permeation chromatography was performed on the pristine polypropylene and on dried polypropylene nanoparticles to test this hypothesis. The number-weighted mean molar mass M_n of (1.1-1.2) × 10^4 g mol^{-1}, the mass-weighted mean molar mass M_w of 3.6 × 10^4 g mol^{-1}, and the dispersity index $Đ$ of 2.9 to 3.3 did not change significantly due to particle preparation, i.e., the main characteristics of the molecular weight distribution remained unchanged. This result strongly indicates that the polypropylene chains themselves stay unchanged during the preparation of nano-polypropylene. It should be noted that PP with a higher molar mass can also be employed for the preparation of PP nanoparticles [16].

2.3 Synthesis of polypropylene nanoparticles

For each batch, 6.0 g of polypropylene granules were added to a tall glass beaker, followed by the addition of 115 mL of acetone. The beaker was cooled in an ice bath to prevent acetone evaporation during preparation. After dispersion, the solution was filtered through a folded filter to remove larger polymer aggregates. Acetone was evaporated until approximately 10% of the liquid remained. Then, 115 mL of water was added to the mixture, and the remaining acetone was evaporated to produce an aqueous dispersion of the polymer nanoparticles. The dispersion was then filtered again using a folded filter to remove any particles that might have aggregated during transfer into water.

In the field of nanotechnology, numerous preparation processes are unsuccessful due to a lack of reproducibility, a concern that could similarly be applicable in this context. Therefore, we conducted a repeatability study to assess the consistency of our particle preparation process. To achieve this, polypropylene nanoparticles were produced 59 times to obtain statistically significant data on the method's consistency. The hydrodynamic diameters were measured for one sample from each batch. We then compared results from different batches using their z-scores.

In this study, z-scores are calculated as $z = \frac{x-\bar{x}}{\sigma}$, with x being the result of the measurand D_h determined for each batch, $\overline{x}$ being the arithmetic mean of the measurand values, and σ being the standard deviation of the mean values. We refer to Lamberty et al. [19] for the application of the z-score in an interlaboratory comparison for the measurement of the particle size and zeta potential of silica nanoparticles in an aqueous suspension. Often, z-scores ranging from -2 to +2 are considered satisfactory, scores in the ± interval between 2 and 3 are questionable, and those outside -3 and +3 are unsatisfactory. We adopted this classification here and found that most values fall within the range of -2 to 2. Finally, 52 batches were accepted and combined into a master batch. From this master batch, a total of 480 samples were placed in glass vials and heated at 90°C for 3 hours. Further details are published elsewhere [16].

2.4 Preparation of reference material

The reference material was prepared following the method described above. The process was repeated multiple times, and all batches displaying a D_h with a z-score between -2 and +2 were combined in a 5 L bottle. The stock bottle was gently swirled to mix the batches. It was equipped with a BRAND seripettor bottle-top dispenser with a 10 mL dispensing volume. The reference material was then dispensed into small screw-top glass bottles. After every 15th fill, the stock bottle was swirled again to ensure thorough mixing. Ultimately, 480 bottles, each containing 10 mL of the reference material, were filled (see Figure 1). To enhance durability, the samples were pasteurized in an oven at 90°C for 3 hours. These samples were subsequently used for all measurements. An example bottle containing BAM-N010 polypropylene nanoparticles and 10 mL of aqueous polypropylene nanoparticle dispersion is shown in Figure 1.

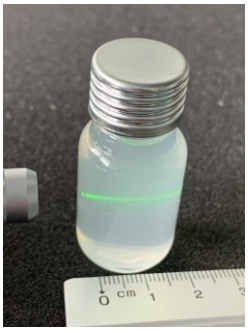

Figure 1: BAM-N010 bottle containing 10 mL of an aqueous dispersion of polypropylene nanoparticles. The dispersion is illuminated from the left with a green laser illustrating its light-scattering properties.

3 Characterization

The hydrodynamic diameter of BAM-N010 was determined with dynamic light scattering in aqueous dispersions with two different devices: Litesizer 500 (Anton Paar AG, follows ISO 22412), here *Device 1*, and ALV 7004 (ALV Langen), here *Device 2*. Details are provided in Section 7.2. An additional measurement series was conducted in

2022 with ZetaSizer Nano ZS (Malvern Panalytical, follows ISO 22412), here *Device 3*. However, in a characterization study, all measurements should be from a similar period and for this reason that older measurement series was excluded from this characterization study.

The dispersions were measured immediately after opening the vials, using 1 mL from each vial, without any additional treatment, at 25°C. Ten randomly selected bottles were measured three times each. The individual results are shown in Table 1. The value D_{char} for the D_h was calculated from the average values D_i obtained from the measurements of devices 1 and 2 and the number of devices p = 2 as

$$D_{char} = \frac{\sum D_i}{p}. \qquad \text{Equation 1}$$

The value determined in this characterization study is D_{char} = 173.9 nm. Mean values for measurements obtained from all three devices are provided in Table 2.

The uncertainty u_{char} associated with the characterization is given by Equation A.4 in [1], which defines the standard uncertainty of the mean of p independent measurements:

$$u_{char} = \frac{1}{\sqrt{p}}\, u_{rep}, \qquad \text{Equation 2}$$

Where u_{rep} represents the standard deviation between instruments or laboratories, reflecting the reproducibility of the measurement process. A direct estimate of u_{rep} can be obtained from the standard deviation of the two instrument readings, yielding 4.6 nm. However, a standard deviation derived from only two measurements is statistically weak and does not provide a reliable estimate of reproducibility.

To obtain a more robust and representative value, we rely on the interlaboratory comparison (ILC) reported in [20]. This study found a relative standard deviation of 7.1 % for nanoPP in water across all participating laboratories and instruments (Table 5 in [20]). When applied to the present measurement scale, this corresponds to an absolute reproducibility uncertainty of 12.4 nm, which is a conservative estimate compared to the directly calculated value of 4.6 nm.

Using the ILC-based reproducibility estimate and p=2, the characterization uncertainty becomes 8.7 nm.

Table 1. Characterization of the hydrodynamic diameters of BAM-N010 with three different DLS devices. Provided are the devices, the sample IDs, and the corresponding D_h values (in nm).

Device 1	ID 1	Dh 1	Device 2	ID 2	Dh 2	Device 3	ID 3	Dh 3
Litesizer 500	243	177.2	ALV 7004	41	180.6	ZetaSizer Nano ZS	88	177.4
Litesizer 500	374	168.5	ALV 7004	61	176.3	ZetaSizer Nano ZS	299	179.0
Litesizer 500	056	178.4	ALV 7004	79	169.4	ZetaSizer Nano ZS	196	174.5
Litesizer 500	249	173.8	ALV 7004	98	176.0	ZetaSizer Nano ZS	150	184.6
Litesizer 500	356	172.6	ALV 7004	142	180.5	ZetaSizer Nano ZS	211	190.4
Litesizer 500	125	168.6	ALV 7004	143	180.0	ZetaSizer Nano ZS	153	188.6
Litesizer 500	312	164.5	ALV 7004	218	183.5	ZetaSizer Nano ZS	133	180.0
Litesizer 500	479	168.3	ALV 7004	257	179.2	ZetaSizer Nano ZS	317	180.8
Litesizer 500	441	167.8	ALV 7004	395	175.1	ZetaSizer Nano ZS	463	177.3
Litesizer 500	241	164.5	ALV 7004	428	173.4	ZetaSizer Nano ZS	287	186.2

Table 2. Mean values of the hydrodynamic equivalent spherical diameter and standard deviation for measurements from three different instruments.

Device	Litesizer 500	ALV 7004	ZetaSizer Nano ZS
$D_{char,\ mean}$	170.4	177.4	181.9
Standard deviation	4.9	4.2	5.3

4 Homogeneity

Ten vials were randomly chosen from the 480 produced vials for a homogeneity study in September 2025. Samples were taken from these vials over three repetitions of DLS measurements with the Litesizer 500, resulting in 30 values for D_h with an overall mean of D_{hom} = 172 ± 6 nm (see Figure 2 and Table 3). We continued the homogeneity study with an analysis of variance test (ANOVA) in accordance with the standard ISO 33405 [1]. Here, the variability of the values is represented by the between-group ($M_{between}$) and within-group (M_{within}) mean squares. These values were used to estimate the standard uncertainties related to the between-bottle standard deviation.

$$s_{bb} = \sqrt{\max\left(\frac{M_{between} - M_{within}}{n_0},\ 0\right)} \qquad \text{Equation 2}$$

where n_0 is the number of observations per group (here n_0 = 3; observation at days 1, 2 and 3). The s_{bb} is 0 if $M_{between} < M_{within}$. Additionally, the repeatability standard deviation is calculated as

$$s_r = \sqrt{M_{within}}$$ Equation 3

The between-bottle and repeatability standard deviations are s_{bb} = 0 nm and s_r = 7.2 nm, respectively (results are summarized in **Table 3**). The small s_{bb}-value indicates no between-bottle effect, as expected since all bottles were filled from the same stock suspension. ANOVA employs a variance-based *F*-test to determine whether the group means are equal. The null hypothesis is that all group means are the same. The null hypothesis cannot be rejected if the calculated *F*-value falls below the critical *F*-value F_{crit}. Following this, no evidence was found to reject the hypothesis that the material is sufficiently homogeneous, because F = 0.38 is lower than F_{crit} = 2.39 (see **Table 4**). The contribution of between-unit variation to the combined uncertainty is equal to the between-unit standard deviation, i.e.

$$u_{bb} = s_{bb}$$ Equation 4

The within sample uncertainty is estimated with

$$u_{\text{wb}} = \sqrt{M_{within}}.$$ Equation 5

M_{within} includes variation due to repeatability and within-sample variation. Therefore, Equation 6 can be regarded as an upper bound for the uncertainty within a sample.

The uncertainty contribution from the homogeneity study is

$$u_{\text{hom}} = \sqrt{u_{\text{bb}}^2 + u_{\text{wb}}^2}$$ Equation 6

The uncertainty contribution from the homogeneity study is therefore, $u_{\text{hom}} = \sqrt{(0\ \text{nm})^2 + (7.2\ \text{nm})^2} = 7.2\ \text{nm}$.

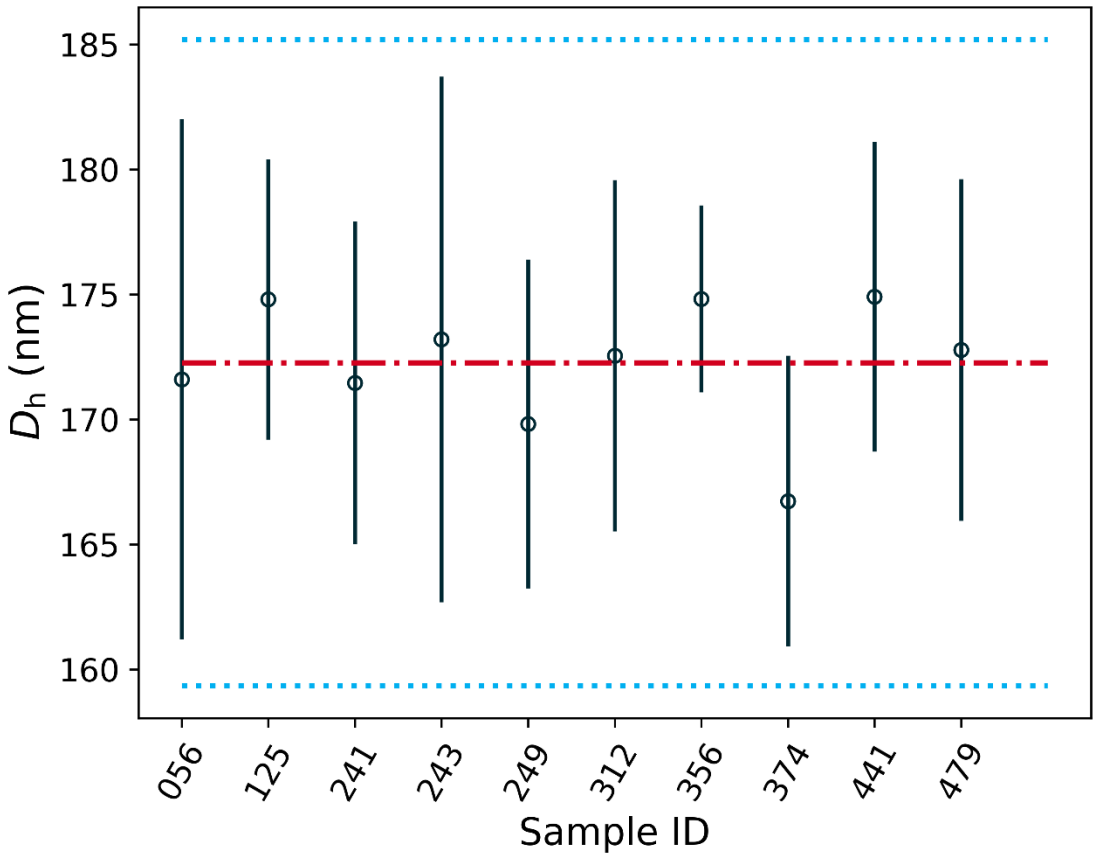

Figure 2. Homogeneity study of the hydrodynamic diameter D_h. The 10 samples included in the study are labeled with their sample IDs. Black circles and error bars show the mean value and standard deviation for each sample. The horizontal red dash-dotted line indicates the overall mean. Blue dotted lines display the uncertainty due to homogeneity $U_{hom} = 2\,u_{hom}$(Eqn.7).

Table 3. Measurement data of the hydrodynamic diameter of the between-unit homogeneity study. Units of Result 1, Result 2, Result 3, Sum, Mean, and Sigma are in nm. Units of SS and Variance are nm^2.

Sample ID	Result 1	Result 2	Result 3	Sum	Mean	SS	Variance	Sigma
056	178.4	159.6	176.8	514.8	171.6	216.4	108.2	10.4
125	168.6	176.4	179.4	524.4	174.8	62.8	31.4	5.6
241	164.5	172.7	177.2	514.4	171.5	83.3	41.7	6.5
243	177.2	161.3	181.2	519.6	173.2	220.9	110.5	10.5
249	173.8	162.2	173.4	509.5	169.8	86.4	43.2	6.6
312	164.5	175.6	177.5	517.6	172.5	98.7	49.3	7.0
356	172.6	179.1	172.7	524.5	174.8	27.9	14.0	3.7
374	168.5	160.2	171.5	500.2	166.7	67.6	33.8	5.8
441	167.8	177.5	179.4	524.7	174.9	76.6	38.3	6.2
479	168.3	169.4	180.6	518.3	172.8	93.3	46.7	6.8

Table 4. ANOVA table for the between-bottle homogeneity study of the hydrodynamic diameter D_h.

Overall Mean (nm)	Overall *s* (nm)	Source of variation	*SS*	*df*	*MS*	*s*	F	F_{crit}	p-value
172	6.4	Between bottles	176	9	19.6	0.0	0.37	2.39	0.93
		Within bottles	1034	20	51.7	7.2			
		Total	1210	29					

5 Stability

The colloidal properties of polypropylene nanoparticles may vary with temperature changes. Therefore, all 480 vials were heated to 90°C for three hours after being filled in January 2022. Any heat sensitivity should be identified quickly through this process. The additional goal of this pasteurization was to reduce bacterial contamination in the vials.

A stability study was conducted from August 2023 (month 0) to May 2026. The samples were stored in the dark at ambient temperatures between 20 °C and 30 °C. At 6 time points, 4 to 10 randomly selected units were measured using the Litesizer 500, with three replicate measurements per unit (see Table 6 in Section 7.3 and Figure 3). For additional context, measurements performed in January 2022 using the Zetasizer Nano are provided. These data are not included in the stability evaluation. Variations between instruments may bias the interpretation of stability trends and therefore must not be considered in the stability assessment. The stability was assessed according to the standard ISO 33405 [1], using a linear regression

$$D_{\text{lts}} = b_0 + b_1 t, \qquad \text{Equation 7}$$

where b_0 is the intercept and b_1 the slope, their estimated standard errors are $s(b_0)$ and $s(b_1)$, respectively. The linear regression provides b_0 = 177 nm, s(b_0) = 2 nm, b_1 = -0.64 nm/month, and $s(b_1)$ = 0.089 nm/month (see solid blue line in **Figure 3**). Next, a test for statistically significant slopes different from zero was conducted. The *t*-test statistics for the slope b_1 significance was calculated using

$$t_{b1} = \frac{|b_1|}{s(b_1)}, \qquad \text{Equation 8}$$

providing t_{b1} = 7.1. The critical value at the 95% confidence level is t_{95} = 2.0 (degrees of freedom = 41). Since $t_{b1} > t_{95}$, there is significance for a slope that differs from zero. Consequently, a significant instability is detected in the hydrodynamic diameter.

Therefore, the contribution of uncertainty of the long-term stability u_{lts} was calculated according to

$$u_{lts} = \sqrt{u_{lts,1}^2 + u_{lts,2}^2} \qquad \text{Equation 9}$$

The first term, according to Eq. (11) in ISO 33405 [1], is

$$u_{lts,1} = s(b_1)(t_m + t_{cert}), \qquad \text{Equation 10}$$

where $s(b_1)$ represents the standard error for the estimated slope, t_m the time interval between value assignment and initial stability monitoring time (24 months), and t_{cert} the period of validity issued (6 months) during that time. This provides $u_{lts,1}$= 2.7 nm.

The second term, according to section 8.7.4 in [1], is

$$u_{lts,2} = \frac{|b_1|}{2\sqrt{3}}(t_m + t_{cert}) \qquad \text{Equation 11}$$

and is applied under the assumption of an equal distribution of the values (rectangular function), providing $u_{lts,2}$ = 5.5nm. Therefore, the uncertainty contribution from the long-term stability is u_{lts} = 6.1. nm.

The slight decrease in the D_h value over time is accompanied by a slight increase in the PDI values from an initial value of 0.09 to around 0.14 at the latest time of the long-term study (see **Figure 4** in Section 7.3). The increase in the PDI indicates a slight change in the particles' size distribution over time, which can be expected for an aqueous dispersion. Possibly, the change in the particles' size distribution could explain the observed decrease in the D_h over time. However, without extensive studies, we can only speculate about the underlying processes. It is important to note here that we can rule out particle aggregation. Even small proportions of aggregates would lead to a massive increase in D_h.

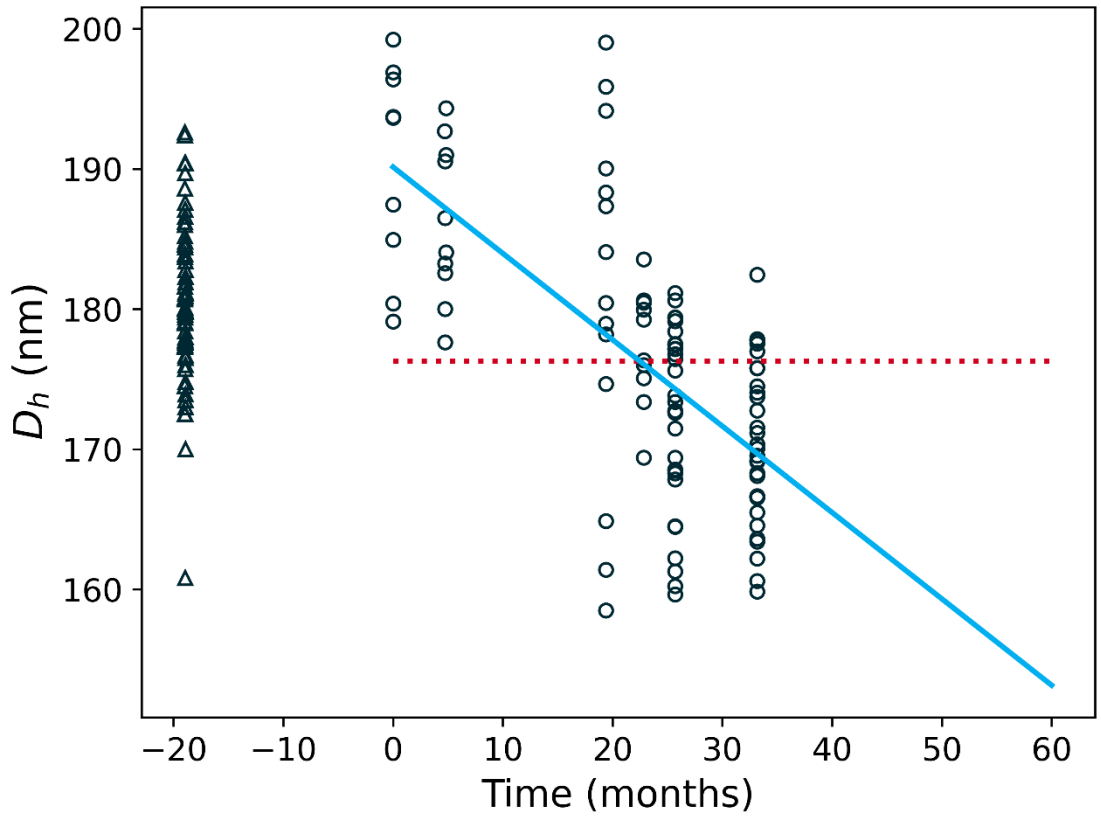

Figure 3. Hydrodynamic diameter of BAM-N010 measured in January 2022 with ZetaSizer Nano ZS (triangles) and between August 2023 and May 2026 with Litesizer 500 (circles). The data from January 2022 were not included in the long-term stability study. The mean value of the Litesizer 500 data is D_h = 176 nm (red dotted line). The blue solid line shows the linear fit of the data. Data is provided in Section 7.3.

6 Combined uncertainty

The hydrodynamic equivalent spherical diameter of BAM-N010 D_{RM} was designated as D_{char}, i.e.,

$$D_{RM} = D_{char} \qquad \text{Equation 123}$$

because no between-unit variation or stability effects need to be regarded. The combined uncertainty u_c was calculated according to Equation 13, using the values of the uncertainty components summarized in **Table 5**. The u_c is a combination of the standard uncertainty contributions due to characterization, homogeneity, and long-term stability.

$$u_c^2 = u_{char}^2 + u_{hom}^2 + u_{lts}^2 \qquad \text{Equation 134}$$

Table 5. Values of uncertainty components for the hydrodynamic diameter of BAM-N010.

D_{RM}	u_{char}	u_{hom}	u_{lts}	u_c	U
174 nm	8.7 nm	7.2 nm	6.1 nm	12.8 nm	26 nm

7 Supporting Information

7.1 Concentration

The mass concentration of polypropylene in water was determined for BAM-N010 as follows: An aluminum open sample pan (for DSC measurements) was weighed empty. It was heated to 150°C on a hot plate. Afterward, a 1 mL aliquot of the sample was added dropwise to the hot pan, ensuring no drops landed outside. The pan was then heated for an additional 15 minutes to remove residual liquid. The pan was weighed again, and the difference was calculated. Gravimetric concentration determination was performed three times. The concentration of polymer in the dispersion was 41 ± 4 mg L^{-1}.

7.2 Experimental for determination of hydrodynamic diameter, PDI, and zeta potential

The light scattering measurements in this study were conducted using three different instruments from three separate manufacturers. The first instrument for DLS and zeta potential measurements is a ZetaSizer Nano ZS (Malvern Panalytical). The samples were filtered through a Millex 0.45 µm PVDF syringe filter. Five measurements, each lasting 10 seconds, were taken for DLS in back-scattering mode at a scattering angle of 173° (2θ). The temperature was maintained at 25°C during all measurements. The instrument follows the ISO standard 22412 for measuring hydrodynamic diameter and polydispersity index [20]. It also complies with ISO standard 13099-2 for zeta potential determination by measuring electrophoretic mobility and applying the Henry equation [21]. An overview of the measurement procedure is provided by Ramaye et al. [22]. In their study, the authors used the same instrument to develop and validate optical methods for assessing the zeta potential of silica and polystyrene particles in aqueous suspensions. In this study, the sample holder was fitted with a folded capillary cell (DTS1070 cell). The zeta potential values represent the average of three measurements, with at least ten runs conducted for each measurement. The second instrument used for determining D_h, PDI, and zeta potential was a Litesizer 500 (Anton Paar AG). The Litesizer 500 complies with ISO standards 22412 and 13092. The third instrument was an ALV 7004 (ALV Langen). It was used for the determination of D_h and PDI. The ALV 7004 instrument complies with the ISO 22412 standard. Measurements for the determination of zeta potential are not possible with the ALV 7004 instrument.

7.3 Data of long-term stability study

The data used for the long-term stability study of Section 5 is given for inspection Table 6.

Table 6. Measurement data of hydrodynamic diameter and PDI of the long-term stability study.

Sample ID	D (nm)	PDI	Date	Time (month)
326	197.5	0.182	2023-08-16	0.0
065	184.3	0.157	2023-08-16	0.0
054	186.4	0.189	2023-08-16	0.0
114	193.7	0.179	2023-08-16	0.0
411	192.7	0.120	2024-01-04	4.7
037	184.6	0.107	2024-01-05	4.7
468	182.2	0.175	2024-01-05	4.7
411	189.8	0.167	2024-01-08	4.8
007	193.4	0.139	2025-03-20	19.4
132	193.7	0.233	2025-03-20	19.4
334	184.0	0.180	2025-03-20	19.4
214	177.3	0.206	2025-03-20	19.4
325	161.6	0.200	2025-03-20	19.4
61	176.3	0.179	2025-07-01	22.8
142	180.5	0.172	2025-07-01	22.8
143	180.0	0.179	2025-07-01	22.8
428	173.4	0.141	2025-07-01	22.8
41	180.6	0.179	2025-07-01	22.8
218	183.5	0.188	2025-07-01	22.8
79	169.4	0.155	2025-07-01	22.8
257	179.2	0.143	2025-07-01	22.8
98	176.0	0.132	2025-07-01	22.8
395	175.1	0.147	2025-07-01	22.8
056	171.6	0.090	2025-09-25	25.7
125	174.8	0.120	2025-09-25	25.7
243	173.2	0.106	2025-09-25	25.7
249	169.8	0.136	2025-09-25	25.7

241	171.5	0.122	2025-09-25	25.7
312	172.5	0.093	2025-09-25	25.7
356	174.8	0.096	2025-09-25	25.7
374	166.7	0.130	2025-09-25	25.7
441	174.9	0.098	2025-09-25	25.7
479	172.8	0.094	2025-09-25	25.7
249	173.4	0.086	2026-05-07	33.1
312	169.3	0.114	2026-05-07	33.1
243	164.1	0.065	2026-05-07	33.1
241	167.5	0.113	2026-05-07	33.1
356	178.0	0.060	2026-05-07	33.1
374	168.0	0.085	2026-05-07	33.1
125	163.2	0.110	2026-05-07	33.1
056	175.2	0.098	2026-05-07	33.1
441	177.1	0.079	2026-05-07	33.1
479	166.5	0.055	2026-05-07	33.1

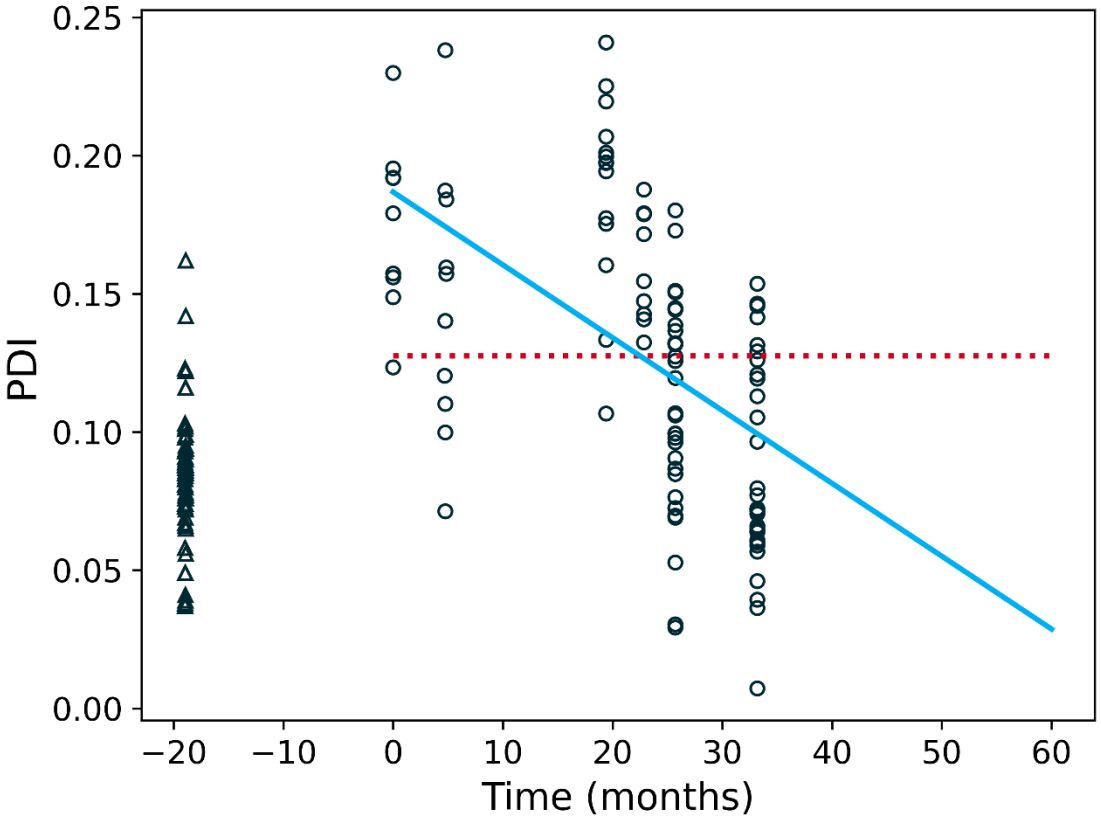

Figure 4. Polydispersity index (PDI) values as a function of time in the long-term stability study (symbols). The mean value is 0.13 ± 0.05 (red dotted line). A linear regression analysis reveals a significant decrease in the PDI with time as PDI = (0.19 ± 0.01) - (2.64 ± 0.4) × 10^{-3} time (in months). The linear increase is indicated as a blue solid line. Data from 2022 (Time = -20 month) were not included in the evaluation.

Additional data not used for the long-term stability study of Section 5 was measured with another instrument model (ZetaSizer Nano ZS by Malvern Panalytical) and it is given for inspection Table 7.

Table 7. Additional measurement data of hydrodynamic diameter and PDI of the long-term stability study.

Sample ID	D (nm)	PDI	Date	Time (month)
11	186.0	0.085	2022-01-24	-19.0
176	172.5	0.049	2022-01-25	-19.0
462	184.8	0.080	2022-01-25	-19.0
211	187.6	0.088	2022-01-25	-19.0
347	177.7	0.039	2022-01-25	-19.0
251	184.4	0.041	2022-01-25	-19.0
317	175.7	0.085	2022-01-25	-19.0
162	177.4	0.091	2022-01-25	-19.0
269	179.0	0.080	2022-01-25	-19.0
287	180.1	0.069	2022-01-25	-19.0

107	177.8	0.102	2022-01-25	-19.0
153	183.9	0.076	2022-01-25	-19.0
133	179.4	0.084	2022-01-25	-19.0
11	189.7	0.090	2022-01-25	-19.0
150	179.6	0.077	2022-01-25	-19.0
13	160.8	0.116	2022-01-25	-19.0
88	186.6	0.066	2022-01-25	-19.0
138	187.1	0.122	2022-01-25	-19.0
463	177.6	0.074	2022-01-25	-19.0
299	178.4	0.087	2022-01-25	-19.0
196	179.8	0.076	2022-01-25	-19.0
463	177.3	0.089	2022-01-24	-19.0
347	181.6	0.058	2022-01-24	-19.0
150	184.6	0.037	2022-01-24	-19.0
211	190.4	0.073	2022-01-24	-19.0
287	186.2	0.088	2022-01-24	-19.0
462	179.1	0.103	2022-01-24	-19.0
299	179.0	0.101	2022-01-24	-19.0
138	180.7	0.123	2022-01-24	-19.0
269	185.2	0.093	2022-01-24	-19.0
196	174.5	0.038	2022-01-24	-19.0
251	192.4	0.073	2022-01-24	-19.0
88	177.4	0.067	2022-01-24	-19.0
107	192.6	0.083	2022-01-24	-19.0
162	183.9	0.049	2022-01-24	-19.0
317	180.8	0.074	2022-01-24	-19.0
153	188.6	0.081	2022-01-24	-19.0
176	172.5	0.091	2022-01-24	-19.0
133	180.0	0.098	2022-01-24	-19.0
13	183.7	0.088	2022-01-24	-19.0
176	170.0	0.077	2022-01-26	-18.9
107	179.8	0.099	2022-01-26	-18.9
269	180.9	0.095	2022-01-26	-18.9
196	173.5	0.085	2022-01-26	-18.9
133	181.1	0.077	2022-01-26	-18.9

150	178.0	0.077	2022-01-26	-18.9
11	173.9	0.088	2022-01-26	-18.9
251	176.0	0.087	2022-01-26	-18.9
13	181.9	0.162	2022-01-26	-18.9
88	182.3	0.056	2022-01-26	-18.9
463	173.0	0.086	2022-01-26	-18.9
153	183.4	0.122	2022-01-26	-18.9
462	181.2	0.142	2022-01-26	-18.9
287	179.9	0.090	2022-01-26	-18.9
347	177.6	0.094	2022-01-26	-18.9
162	182.8	0.076	2022-01-26	-18.9
299	176.5	0.116	2022-01-26	-18.9
211	174.8	0.072	2022-01-26	-18.9
317	176.7	0.065	2022-01-26	-18.9
138	190.4	0.078	2022-01-26	-18.9

7.4 Heat sterilization

Customers often require that reference materials be sterilized, for example, prior to toxicological experiments. Therefore, a test was conducted in June 2025 to sterilize the BAM-N010 samples, which had proven stable over 40 months. Ten randomly selected vials were heat sterilized at 121°C for 90 minutes. DLS and zeta potential measurements of samples from all vials were measured before, three hours after, and 24 hours after sterilization. An overview of the hydrodynamic diameters, PDI values, and zeta potentials is provided in Figure 5 and Table 8. Of importance is that the low values of the zeta potential around -39 mV could explain the colloidal long-term stability of the polypropylene nanoparticles, as well as the thermal stability [15].

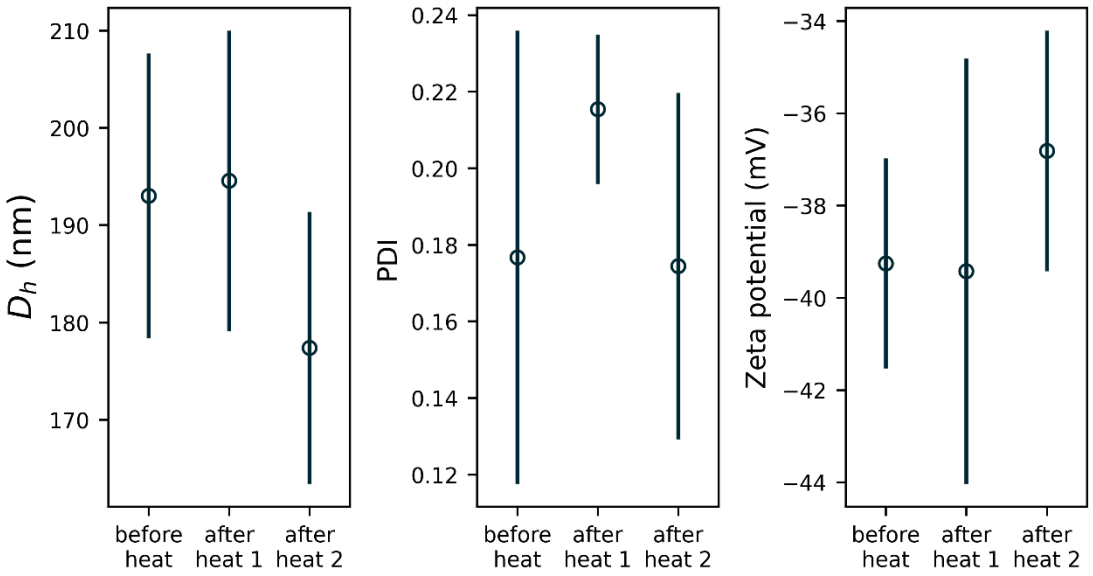

Figure 5. Hydrodynamic diameter, PDI, and zeta potential before heat treatment at 121°C for 90 minutes, 3 hours later, and 24 hours after heat treatment. Symbols represent the mean of 10 measurements, and error bars represent the standard deviation.

Table 8. Data on hydrodynamic diameter, PDI, and zeta potential, and their uncertainties. Data are visualized in Figure 5.

date of measurement	time	D (nm)	u_D (nm)	PDI	u_{PDI}	Zeta potential (mv)	u_{zeta} (mV)
2025-06-30	before sterilization	193	15	0.18	0.06	-39	2
2025-06-30	3 h after sterilization	195	15	0.22	0.02	-39	5
2025-07-07	24 h after sterilization	177	14	0.17	0.05	-37	3

7.5 Scanning electron microscopy (SEM)

SEM was conducted using a Zeiss Supra 40 Scanning Electron Microscope (Zeiss, Oberkochen, Germany), at 10 kV acceleration voltage, 4.8 mm WD, in SE InLens mode, and at various magnifications. Before taking the measurement, the flask containing polypropylene nanoparticles was gently shaken. 3 µL of the suspension (PP, ID336) was drop-cast onto the carbon tape and allowed to dry for approximately 24 hours under laboratory conditions. SEM measurements of the polypropylene nanoparticles were conducted to gain insights into their shapes. A typical SEM image is shown in Figure 6. The particles have distinct fracture edges and appear elongated. Assuming a simplified cylinder geometry allows us to calculate a hydrodynamic equivalent diameter. For this, we set the diffusion coefficient of a sphere to $D_s = k_B T/(3\pi\eta D_h)$, matching that of a cylinder of [23, 24]

$$D_c = \frac{k_B T}{3\pi\eta l}(\log(p) + \nu), \qquad \text{Equation 14}$$

with $p = l/d$ and $\nu = 0.312+0.565p^{-1} - 0.1p^{-2}$, resulting in

$$D_h = \frac{\mathrm{l}}{0.313 - 0.1\mathrm{d}^2/\mathrm{l}^2 + 0.565\mathrm{d}/\mathrm{l} + \log(\mathrm{l}/\mathrm{d})}. \qquad \text{Equation 15}$$

The Boltzmann constant k_B, temperature T, and viscosity η are constants, meaning D_h is determined by the length l and diameter d of the cylinder. Inserting a cylinder with a length of l = 300 nm and a diameter of d = 100 nm results in a hydrodynamic equivalent diameter of D_h = 189 nm. This value aligns with the experimentally observed hydrodynamic diameters, indicating that the SEM image accurately represents the polypropylene nanoparticles. Radiation damage caused by the SEM cannot be ruled out. Nevertheless, the SEM image serves as a reasonable indicator for the particles' shape and size.

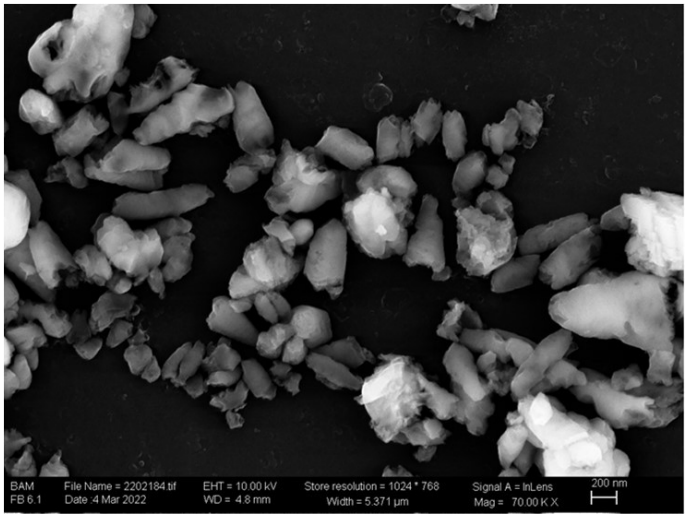

Figure 6. Scanning electron micrograph of polypropylene nanoparticles (scale bar = 200 nm, see also [16]).

8 Information on the proper use of the RM

8.1 Recommended use

The purpose of the polypropylene nanoparticles is to assess and validate analytical techniques for the characterization of polymeric nanoparticles in aqueous environments. We refer to [25, 26] and references therein for a description of the current state of nanoplastics detection.

8.2 Transport, storage, and handling

RM BAM-N010 can be shipped at room temperature. It should be stored in dark, dry conditions at ambient temperature in its original tightly sealed bottle. BAM cannot be responsible for changes that occur during storage at the customer's location, especially in open bottles. During transport, the packaging should be free of plastic to prevent contamination.

8.3 Shelf-life

Based on the available stability data, the reference material is considered fit for use for a period of 6 months from the date of issue of the certificate, provided that it is stored at ambient temperature under the recommended conditions. The stability of the material will continue to be monitored as part of an ongoing stability monitoring program.

8.4 Safety information

The usual laboratory safety precautions for handling liquids must be followed. No hazardous effects are anticipated when the material is used under typical conditions for analyzing aqueous nanoparticle dispersions. It is strongly recommended to handle and dispose of the reference material according to the hazardous materials guidelines legally in force at the site of use and disposal.

9 Information on and purchase of the RM

The reference material, BAM-N010 polypropylene nanoparticles, is supplied by:

Bundesanstalt für Materialforschung und -prüfung (BAM)

Unter den Eichen 87

12205 Berlin, Germany

Orders can be placed at https://www.webshop.bam.de

Each sample of BAM Polypropylene nanoparticles will be distributed together with a detailed report containing the parameter values and their uncertainties, the mean values and standard deviations of all accepted data sets, and information on the analytical methods used.

Information on BAM reference materials is available on the BAM website at https://www.bam.de.

10 References

[1] International Organization for Standardization, *ISO 33405:2024(en) Reference materials — Approaches for characterization and assessment of homogeneity and stability,* **2024**. Geneva, Switzerland.

[2] Wagner, S. & Reemtsma, T., Things we know and don't know about nanoplastic in the environment, *Nature Nanotechnology,* **2019**, *14***,** 300–301.

[3] Cottom, J. W., Cook, E. & Velis, C. A., A local-to-global emissions inventory of macroplastic pollution, *Nature,* **2024**, *633***,** 101–108.

[4] Geyer, R., Jambeck, J. R. & Law, K. L., Production, use, and fate of all plastics ever made, *Science Advances,* **2017**, *3***,** e1700782.

[5] Hartmann, N. B., Huffer, T., Thompson, R. C., Hassellov, M., Verschoor, A., Daugaard, A. E., Rist, S., Karlsson, T., Brennholt, N., Cole, M., Herrling, M. P., Hess, M. C., Ivleva, N. P., Lusher, A. L. & Wagner, M., Are We Speaking the Same Language? Recommendations for a Definition and Categorization Framework for Plastic Debris, *Environmental Science & Technology,* **2019**, *53***,** 1039–1047.

[6] Paul, M. B., Fahrenson, C., Givelet, L., Herrmann, T., Loeschner, K., Böhmert, L., Thünemann, A. F., Braeuning, A. & Sieg, H., Beyond microplastics - investigation on health impacts of submicron and nanoplastic particles after oral uptake in vitro, *Microplastics and Nanoplastics,* **2022**, *2***,** 1–16.

[7] Paul-Pont, I., Tallec, K., Gonzalez-Fernandez, C., Lambert, C., Vincent, D., Mazurais, D., Zambonino-Infante, J. L., Brotons, G., Lagarde, F., Fabioux, C., Soudant, P. & Huvet, A., Constraints and Priorities for Conducting Experimental Exposures of Marine Organisms to Microplastics, *Frontiers in Marine Science,* **2018**, *5***,** 1–22.

[8] Frere, L., Paul-Pont, I., Rinnert, E., Petton, S., Jaffre, J., Bihannic, I., Soudant, P., Lambert, C. & Huvet, A., Influence of environmental and anthropogenic factors on the composition, concentration and spatial distribution of microplastics: A case study of the Bay of Brest (Brittany, France), *Environmental Pollution,* **2017**, *225***,** 211–222.

[9] Gigault, J., ter Halle, A., Baudrimont, M., Pascal, P. Y., Gauffre, F., Phi, T. L., El Hadri, H., Grassl, B. & Reynaud, S., Current opinion: What is a nanoplastic?, *Environmental Pollution,* **2018**, *235***,** 1030–1034.

[10] Tallec, K., Huvet, A., Di Poi, C., Gonzalez-Fernandez, C., Lambert, C., Petton, B., Le Goic, N., Berchel, M., Soudant, P. & Paul-Pont, I., Nanoplastics impaired oyster free living stages, gametes and embryos, *Environmental Pollution,* **2018**, *242***,** 1226–1235.

[11] Hollóczki, O. & Gehrke, S., Can Nanoplastics Alter Cell Membranes?, *ChemPhysChem,* **2020**, *21***,** 9–12.

[12] Hollóczki, O. & Gehrke, S., Nanoplastics can change the secondary structure of proteins, *Scientific Reports,* **2019**, *9***,** 1–7.

[13] Ekvall, M. T., Lundqvist, M., Kelpsiene, E., Šileikis, E., Gunnarsson, S. B. & Cedervall, T., Nanoplastics formed during the mechanical breakdown of daily-use polystyrene products, *Nanoscale Advances,* **2019**, *1***,** 1055–1061.

[14] Ekvall, M. T., Gimskog, I., Hua, J., Kelpsiene, E., Lundqvist, M. & Cedervall, T., Size fractionation of high-density polyethylene breakdown nanoplastics reveals different toxic response in Daphnia magna, *Scientific Reports,* **2022**, *12***,** 3109.

[15] Bhattacharjee, S., DLS and zeta potential - What they are and what they are not?, *Journal of Controlled Release,* **2016**, *235***,** 337–351.

[16] Hildebrandt, J. & Thünemann, A. F., Aqueous Dispersions of Polypropylene: Toward Reference Materials for Characterizing Nanoplastics, *Macromolecular Rapid Communications,* **2023**, *44***,** 2200874.

[17] Lionetto, F., Corcione, C. E., Rizzo, A. & Maffezzoli, A., Production and Characterization of Polyethylene Terephthalate Nanoparticles, *Polymers,* **2021**, *13***,** 3745.

[18] Haynes, W. M., *Handbook of Chemistry and Physics (97th Edition),* **2016–2017**.

[19] Lamberty, A., Franks, K., Braun, A., Kestens, V., Roebben, G. & Linsinger, T. P. J., Interlaboratory comparison for the measurement of particle size and zeta potential of silica nanoparticles in an aqueous suspension DISCUSSION, *Journal of Nanoparticle Research,* **2011**, *13***,** 7317–7329.

[20] International Organization for Standardization, *ISO 22412:2017(E) , Particle size analysis - Dynamic light scattering (DLS),* **2017**. Geneva, Switzerland.

[21] International Organization for Standardization, *ISO 13099-2: Colloidal systems - Methods for zeta-potenital determination - Part 2: Optical Methods,* **2012**. Geneva, Switzerland, ISO.

[22] Ramaye, Y., Dabrio, M., Roebben, G. & Kestens, V., Development and Validation of Optical Methods for Zeta Potential Determination of Silica and Polystyrene Particles in Aqueous Suspensions, *Materials,* **2021**, *14***,** 290.

[23] Delatorre, J. G., Martinez, M. C. L. & Tirado, M. M., DIMENSIONS OF SHORT, RODLIKE MACROMOLECULES FROM TRANSLATIONAL AND ROTATIONAL DIFFUSION-COEFFICIENTS - STUDY OF THE GRAMICIDIN DIMER, *Biopolymers,* **1984**, *23***,** 611–615.
[24] Pecora, R., Dynamic light scattering measurement of nanometer particles in liquids, *Journal of Nanoparticle Research,* **2000**, *2***,** 123–131.
[25] Caldwell, J., Taladriz-Blanco, P., Lehner, R., Lubskyy, A., Ortuso, R. D., Rothen-Rutishauser, B. & Petri-Fink, A., The micro-, submicron-, and nanoplastic hunt: A review of detection methods for plastic particles, *Chemosphere,* **2022**, *293***,** 133514.
[26] Mitrano, D. M., Wick, P. & Nowack, B., Placing nanoplastics in the context of global plastic pollution, *Nature Nanotechnology,* **2021**, *16***,** 491–500.

11 Annexes

11.1 Information about the software utilized

Data processing and analysis were implemented using the Python programming language, version 3.8.5, for 64-bit systems on Windows 10 (available at https://www.python.org). The Python modules SciPy (version 1.6.3, https://scipy.org), NumPy (1.19.2, https://numpy.org), pandas (1.1.3, https://pandas.pydata.org), Matplotlib (3.4.3, https://matplotlib.org) were used for calculations. JupyterLab (Version 2.2.6, https://jupyter.org) was used as a user interface.

11.2 Acknowledgment

The author acknowledges Jana Hildebrandt's immense contributions in realizing this reference materials project. Thanks are due to Malte Wulff for helping with the adaptation of the preparation method and to Tina Rybak, Maximilian Ebisch, and Kai Simon Rother for assisting with the preparation of the nanoplastics samples. In addition, the authors thank Ralf Bienert for assistance with the zeta potential measurements, Jana Falkenhagen and Karin Böttcher for performing the AF4 and GPC measurements, and Vasile-Dan Hodoroaba and Dmitri Ciornii for carrying out the SEM measurements. Thanks go to Sebastian Recknagel and Vasile-Dan Hodoroaba for reviewing the manuscript.